High output performance of piezoelectric energy harvesters using epitaxial Pb(Zr, Ti)O3 thin film grown on Si substrate

Kim, Eun-Ji ; Kweon, Sang-Hyo ; Nahm, Sahn ; Sato, Yukio ; Tan, Goon ; Kanno, Isaku

(Citation)
Applied Physics Letters,121(16):161901

(Issue Date)
2022-10-17

(Resource Type)
journal article

(Version)
Accepted Manuscript

High output performance of piezoelectric energy harvesters using epitaxial $Pb(Zr, Ti)O_3$ thin film grown on Si substrate

Eun-Ji Kim[1], Sang-Hyo Kweon[2], Sahn Nahm[1], Yukio Sato[3], Goon Tan[4,a)], and Isaku Kanno[2,a)]

AFFILIATIONS

[1]Department of Materials Science and Engineering, Korea University, 145 Anam-ro, Seongbuk-gu, Seoul 02841, Republic of Korea

[2]Department of Mechanical Engineering, Kobe University, 1-1 Rokkodai-cho, Nada-ku, Kobe 657-8501, Japan

[3]Department of Materials Science and Engineering, Kyushu University, 744 Motooka, Nishi-ku, Fukuoka 819-0395, Japan

[4]Division of Physics, Faculty of Liberal Arts, Sciences and Global Education, Osaka Metropolitan University, 1-1 Gakuen-cho, Nakaku, Sakai, Osaka 599-8531, Japan

[a)]**Authors to whom correspondence should be addressed:** tan@omu.ac.jp and kanno@mech.kobe-u.ac.jp

ABSTRACT

For a high power density in piezoelectric energy harvesters, both a large direct piezoelectric coefficient ($e_{31,f}$) and a small relative permittivity constant ($\varepsilon_{r,33}$) are required. This study proposed an energy harvesting device made of an epitaxial Pb(Zr, Ti)O_3 (PZT) thin film grown on a Si substrate. The epitaxial PZT thin film is deposited on the Si substrate by RF magnetron sputtering. The epitaxial PZT thin film grown on Si substrate has a $\varepsilon_{r,33}$ constant of 318. The output voltage as a function of input displacement was measured using a shaker to evaluate the direct $e_{31,f}$ coefficients and energy harvester output characteristics. According to the figure of merit (FOM) defined as $(e_{31,f})^2/\varepsilon_0\varepsilon_{r,33}$, the epitaxial PZT/Si cantilever is 32 GPa. At a resonant frequency of 373 Hz under an acceleration of 11 m/s^2, the epitaxial PZT/Si cantilever has a high output power of 40.93 μW and power density of 108.3 μW/cm^2/g^2 without any damage, which is very promising for high power energy harvester applications.

With the increasing demand for Internet of Things systems, wireless sensor technologies that enable wireless communication between electronic devices are also being developed.[1,2] However, because of the limited battery life, self-powered systems are required, as well as low-power circuit technology or an ecofriendly alternative energy source. In particular, energy harvesters made of piezoelectric materials like Pb(Zr, Ti)O_3 (PZT) have several advantages, including structural simplicity, high energy conversion efficiency, and high power density.[3-6] They are suitable for the miniaturization of devices.

It is important to evaluate the piezoelectric material energy conversion efficiency for piezoelectric energy harvesters (PEHs). Appropriate piezoelectric materials must be used to generate the maximum output electrical energy for PEHs to improve energy conversion efficiency. The figure of merit (FOM) can be used to understand the relationship between the piezoelectric properties of materials and the output power of PEHs.[7,8] For an energy harvester using a piezoelectric thin film, the FOM is known as $(e_{31,f})^2/\varepsilon_0\varepsilon_{r,33}$, where $e_{31,f}$, ε_0, and $\varepsilon_{r,33}$ are the effective transverse piezoelectric constant, dielectric constant of vacuum, and relative permittivity constant, respectively.[9] According to the FOM, a higher power density requires a large $e_{31,f}$ coefficient and small $\varepsilon_{r,33}$. The epitaxial thin films are good candidates for energy harvesters because they have low defects, stable performance, low relative permittivity constant, and high ferroelectric and piezoelectric properties.[10-12] According to the thermodynamic calculations, the PZT thin films with the largest degree of *c*-axis orientation showed the highest remanent polarization values and the lowest dielectric constants.[11,12] Epitaxial piezoelectric thin films are typically grown on single oxide crystals such as MgO or $SrTiO_3$ substrates.[13-15] Our previous study demonstrated the epitaxial PZT thin films on stainless steel substrates for energy harvesting applications using the laser lift-off (LLO) transfer technology. The epitaxial PZT thin films were initially grown on MgO

single crystal substrates.[16] However, Si is a standard material for fabricating microelectromechanical system (MEMS) devices. Hence, there is a growing demand for integrating high-oriented or epitaxial functional thin films on Si substrates. So far, several studies on the epitaxial growth of PZT thin films on Si substrates have been reported.[17,18] Nevertheless, there are not sufficient reports of the detailed piezoelectric characterizations of the epitaxial PZT thin films grown on Si substrates. In this study, we have deposited the epitaxial PZT thin film on (001)SRO/Pt/ZrO_2/Si substrate. In particular, (001)SRO/Pt/ZrO_2 bottom layers on Si indicate high electrical conductivity through the inclusion of Pt and is a more practical film structure compared to previous studies using SRO/CeO_2/YSZ/Si(100) and SRO/STO/Si(100) substrates.[17,18]

Accurate piezoelectric coefficient measurements are also critical for predicting the final performance of devices fabricated with MEMS technology. The effective transverse piezoelectric coefficient ($e_{31,f}$) is commonly used as an important piezoelectric coefficient for characterizing piezoelectric applications such as actuators and harvesters.[19,20] Direct and converse piezoelectric effects are the basis for measuring piezoelectric properties.[19,21,22] It is noted that the $e_{31,f}$ coefficients of piezoelectric thin films could differ from the direct piezoelectric and converse piezoelectric effects.[22] Considering the operation of an energy harvester, the direct $e_{31,f}$ coefficients are preferable for discussing the FOM and estimating the power performance of piezoelectric thin films.[23,24] However, the converse $e_{31,f}$ coefficients are typically used for evaluating the FOM of PEHs in previous studies.[25,26] Thus, a system for precisely evaluating the direct $e_{31,f}$ coefficients must be developed to discuss the FOM. This study proposes a method for measuring the direct piezoelectric coefficient that uses a shaker. In this system, direct $e_{31,f}$ coefficients and output characteristics of the energy harvester can be measured simultaneously.

In this work, epitaxial PZT thin film was deposited on Si substrates with buffered layers. Then

unimorph cantilever composed of the epitaxial PZT thin film on Si substrate (PZT/Si) was fabricated to measure the output performance of the energy harvester. A measurement method of direct $e_{31,f}$ coefficients was used to evaluate the output performance of the epitaxial PZT/Si cantilever. Therefore, we found that the epitaxial PZT thin film grown on Si substrate is very suitable for use in high-performance energy harvesters. The epitaxial growth of the PZT thin films on Si substrates would give a big impact for piezoelectric MEMS technologies which mainly use polycrystalline PZT thin films on Si today.

PZT thin film with a Zr/Ti ratio of 48/52 was deposited on the epitaxial (001)SRO/Pt/ZrO_2/Si substrate by RF magnetron sputtering. The thicknesses of the epitaxial SRO-coated Si substrate and PZT thin film were 725 and 2.5 μm, respectively. The structural properties of the PZT thin film were determined using X-ray diffraction (XRD, SmartLab, Rigaku, Japan) and transmission electron microscopy (TEM). Relative permittivity constant ($\varepsilon_{r,33}$) and dielectric loss (tan δ) of the PZT thin film were measured using an LCR meter (IM 3536 LCR meter, HIOKI, Japan). The polarization–electric field (P–E) hysteresis curve was obtained using a ferroelectric tester (Precision Multiferroic II, RADIANT TECHNOLOGIES, INC., USA). Further details are provided in sections 1.1 and 1.2 of the Supplementary material. The $e_{31,f}$ coefficients from converse and direct effect and output performance of epitaxial PZT/Si cantilever were measured using the cantilever method. We cut the specimens into rectangular beams along the ⟨110⟩Si directions. The dimensions of the cantilever are 2 mm in width and about 15 mm in length. Details of the measurement methods are given in sections 1.3 and 1.4 of the Supplementary material.

Figure 1(a) shows the XRD pattern of PZT thin film deposited on (001)SRO/Pt/ZrO_2/Si substrate. The XRD pattern showed strong peaks of {001} and {002} PZT without any other phases. We also performed a reciprocal space map (RSM) analysis of the PZT thin film on the

(001)SRO/Pt/ZrO_2/Si substrate, as shown in Figure 1(b). In the RSMs of the PZT thin film around the PZT *004* [Figure 1(b)] and PZT *204* (Figure S1) reflections, only spotty PZT peaks are observed. This indicates that the PZT thin film was epitaxially grown on (001)SRO/Pt/ZrO_2/Si substrate. We also observed the *a*-domains (PZT *400*) spots as three separated spots in Figure 1(b). Several studies using crystal structure analysis have reported a similar domain structure.[27,28] The tilted domains in a PZT tetragonal structure are geometrically caused by the 90° domain with the {101} domain wall.[27] Furthermore, from the peak positions of PZT *004* and PZT *204*, the lattice constants of *a* and *c* were calculated as 4.08 and 4.14 Å, respectively. This indicates that the *c*/*a* ratio is 1.01, which means that the PZT thin film on the (001)SRO/Pt/ZrO_2/Si substrate has a tetragonal structure. The scanning transmission electron microscopy (STEM) analysis was also conducted on the PZT thin film grown on the (001)SRO/Pt/ZrO_2/Si substrate to confirm the domain structure of the thin film. An enlarged high-resolution scanning transmission electron microscopy (HRSTEM) image of the PZT thin film on (001)SRO/Pt/ZrO_2/Si substrate shows (100) and (001) lattice fringes, as shown in Figure 1(c). We confirmed that the lattice parameter values of (100) and (001) directions were 4.06 and 4.16 Å, respectively. It shows that the *c*/*a* ratio is close to the value obtained from the RSM estimation. The inset image shows the electron diffraction pattern of the crystalline PZT phase, which shows the (100) and (001) reflections, suggesting that the PZT thin film has good crystallinity. These results confirmed that the PZT thin film grows epitaxially on the (001)SRO/Pt/ZrO_2/Si substrate with a tetragonal structure.

The relative permittivity constant ($\varepsilon_{r,33}$) and dielectric loss (tan δ) value of the epitaxial PZT thin film on Si substrate were 318 and 0.01, respectively. According to the polarization–electric field (*P*–*E*) hysteresis loop measurement (Figure S2), the epitaxial PZT thin film exhibits ferroelectric properties with a well-saturated square-shape hysteresis loop. The epitaxial PZT thin film on the

Si substrate had a remanent polarization (P_r) value of 48.6 μC/cm^2. The epitaxial PZT thin film on the Si substrate showed a large P_r value because of the dominant *c*-axis orientation.

The $e_{31,f}$ coefficients of the epitaxial PZT/Si cantilever evaluated from the converse and direct piezoelectric effect were measured using the cantilever method, and the details of the measurement method are mentioned in sections 1.3 and 1.4 of the Supplementary material. The setup for measuring the converse $e_{31,f}$ coefficients is shown in Figure 2(a). To evaluate the converse $e_{31,f}$ coefficients of the epitaxial PZT/Si cantilever, the output tip displacement was measured using a laser Doppler vibrometer by applying a negative unipolar sinusoidal voltage from 5 to 20 V_{pp} at a frequency of 600 Hz. For measuring the direct $e_{31,f}$ coefficients of the epitaxial PZT/Si cantilever, we confirmed the output voltage using an oscilloscope as a function of the input tip displacement generated by the shaker at resonant frequency [Figure 2(b)].

Figure 3 shows the output tip displacements and converse $|e_{31,f}|$ coefficients of the epitaxial PZT/Si cantilever as a function of applied voltage. The output tip displacement of the epitaxial PZT/Si cantilever increased proportionally with the applied voltage, as shown in Figure 3(a). From the output displacement (δ_{out}) generated by the input voltage (V_{in}), the converse $|e_{31,f}|$ coefficients of the epitaxial PZT/Si cantilever were calculated using the following equation:

$$e_{31,f} = -\frac{E_s h_s^2}{3l^2(1 - v_s)} \cdot \frac{\delta_{out}}{V_{in}}, \quad (1)$$

where E_s, h_s, and v_s represent Young's modulus, thickness, and Poisson's ratio of the substrate, respectively, and l represents the length of the unimorph cantilever. We used the values of E_s and v_s of <110> Si as 170 GPa and 0.064, respectively.[29] The derivation of Equation 1 is reported in detail in our previous study.[22] The calculated converse $|e_{31,f}|$ values of the epitaxial PZT/Si cantilever are almost constant, regardless of the applied voltage, and are in the range of 14.0–14.3

C/m^2, as shown in Figure 3(b). This implies that the as-grown PZT thin film is fully polarized in the thickness direction. The results of the converse piezoelectric coefficients measured by applying 1st, 2nd, and 3rd voltages to the epitaxial PZT/Si cantilever were shown in Figure S3. We observed constant and stable values of the converse $e_{31,f}$ coefficients under the application of repeated voltages. The epitaxial PZT/Si cantilever has a higher converse $|e_{31,f}|$ coefficients than the polycrystalline PZT/Si cantilever reported in other studies.[22,30,31] It is considered that the high crystal orientation of the {001} plane of the epitaxial PZT thin film contributes to improving the piezoelectric coefficients.[32] Therefore, the epitaxial PZT/Si cantilever is expected to improve the performance of devices such as actuators that use the converse effect.

Figure 4 shows the direct piezoelectric coefficients $|e_{31,f}|$ of the epitaxial PZT/Si cantilever evaluated from the output voltage as a function of the input displacement at a resonant frequency. The output voltage of the epitaxial PZT/Si cantilever increased proportionally with the input displacement, as shown in Figure 4(a). The direct $e_{31,f}$ coefficients were calculated using Equation 2 (for derivation, see section 5 of the Supplementary material) from the relationship between the input tip displacement (δ_{in}) and the output voltage (V_{out}):

$$e_{31,f} = \frac{\{4l_a^{\,2} + 3l_a(l_b - l_a)\}C\sqrt{1 + (\omega_s C R_{load})^{-2}}}{3(1 - \nu_s)h_s\{l_a + (l_b - l_a)\}w} \cdot \frac{V_{out}}{\delta_{in}}, \quad (2)$$

where $l_{a,b}$ and w represent the length and width of the unimorph cantilever, respectively; h_s and ν_s represent the thickness and Poisson's ratio of the substrate, respectively (Figure S4); ω_s represents an angular frequency ($\omega_s = 2\pi f$); C represents the capacitance of the piezoelectric thin film, and R_{load} is the load resistance of an oscilloscope input impedance (R_{load} = 1 MΩ). The capacitance of the epitaxial PZT/Si cantilever is 32.4 nF. To calculate the direct $e_{31,f}$ values, the Poisson's ratio of <110> Si was 0.064. The direct $|e_{31,f}|$ values of the epitaxial PZT/Si cantilever were calculated to

be 9.3–9.5 C/m^2 at a resonant frequency of 373–375 Hz, as shown in Figure 4(b). These values were less than the converse $|e_{31,f}|$ values of the epitaxial PZT/Si cantilever, as shown in Figure 3(b). This is due to the lack of extrinsic contribution, such as domain motion.[22] Additionally, the direct $|e_{31,f}|$ values of the epitaxial PZT/Si cantilever were higher than the epitaxial PZT/MgO cantilever.[22] Thus, it was found that epitaxial PZT thin film on Si substrate is suitable for use in piezoelectric sensors or energy harvester applications.

Figure 5 shows the output performance of PEHs using the epitaxial PZT/Si cantilever. Using the measurement system of direct $e_{31,f}$ coefficients [Figure 2(b)], we measured the output power of the epitaxial PZT/Si cantilever at a resonant frequency. First, the output power and voltage were measured as a function of load resistance at a resonant frequency of 374 Hz and an acceleration of 3 m/s^2, as shown in Figure 5(a). The output voltage increases with the load resistance, and the output electric power [$P = V^2/R$] has a maximum value of 3.6 μW at the load resistance of approximately 13 kΩ. The optimal load resistance (R_{opt}) was obtained from $1/(\omega C)$, where ω and C represent the natural angular frequency and capacitance of the energy harvester, respectively, and the calculated R_{opt} (13.06 kΩ) was consistent with the experimental results. Furthermore, we evaluated the acceleration dependence of the output power with an optimal load resistance at a resonant frequency, as shown in Figure 5(b). The resonant frequency slightly decreases from 375 to 373 Hz, depending on the acceleration, owing to the softening effect of the spring constant of the unimorph cantilever (Figure S5).[33] The output power increases with acceleration, reaching 40.93 μW at 11 m/s^2 with an input displacement of 151 μm without damaging the cantilever. The normalized power density was also calculated as the square of the acceleration and the area of the epitaxial PZT/Si cantilever. Figure S6 shows the calculated power density value is 108.3 μW/cm^2/g^2 at 11 m/s^2. Furthermore, we estimated the mechanical stress of the epitaxial PZT/Si

cantilever at the maximum acceleration of 11 m/s^2 using Equation S15 in section 5 of the Supplementary material. The calculated value is approximately 120 MPa. According to Coleman *et al.,* the crack initiation stress was about 500 MPa.[34] The maximum stress at an acceleration of 11 m/s^2 in our study was smaller than the crack initiation stress. Furthermore, we considered the relationship between the output power and acceleration based on the theoretical study from Morimoto *et al*.[35] Theoretically, the output power increases with the square of the acceleration according to Equation S20 in section 6 of the Supplementary material, and it is shown as a dashed line in the graph, as shown in Figure 5(b). As a result, the experimental values are relatively consistent with the theoretical values. In addition, the output power was repeatedly measured to evaluate the reliability and durability of energy harvester performance, as shown in Figure S7. We confirmed that the output power was constant and stable under the same conditions.

Considering the operation of the energy harvester, the direct $e_{31,f}$ coefficients are preferred for discussing the FOM and estimating the output power performance of piezoelectric thin films. Thus, we calculated the FOM of the epitaxial PZT/Si cantilever using the converse $e_{31,f}$ coefficients as well as direct $e_{31,f}$ coefficients to compare with other studies (summarized in Table I).[22,25,30,31,36-38] As a result, the FOM values of the epitaxial PZT/Si cantilever calculated from the converse and direct $e_{31,f}$ coefficient are 70–73 and 32 GPa, respectively. From the perspective of energy harvesters, our FOM value calculated from direct $e_{31,f}$ coefficient is sufficiently high, as seen in Table I. The measurement methods in this study are appropriate and practical for actuators and energy harvester devices.

We investigated the piezoelectric coefficients of the epitaxial PZT/Si cantilever from the direct and converse piezoelectric effects. The converse and direct $|e_{31,f}|$ values were estimated as 14.0–14.3 C/m^2 and 9.3–9.5 C/m^2, respectively, and their relative permittivity constant was 318. The

FOM value of the epitaxial PZT/Si cantilever evaluated from the direct piezoelectric effect was calculated as 32 GPa. The epitaxial PZT/Si cantilever has a high output power of 40.93 μW and power density of 108.3 $\mu W/cm^2/g^2$ without any damage at a resonant frequency of 373 Hz under an acceleration of 11 m/s^2. These evaluations indicate that the power generation performance of the epitaxial PZT/Si harvester is significantly superior. Therefore, it is suggested that the epitaxial PZT thin film on Si substrate has a high potential for use as high-performance energy harvesters.

SUPPLEMENTARY MATERIAL

See supplementary material for the complete experimental section and other characterization results.

ACKNOWLEDGMENT

This work was supported by JST-CREST (grant no. JPMJCR20Q2) and BK21 FOUR Program through the National Research Foundation of Korea (NRF) funded by the Ministry of Education (4199990514635). TEM and STEM analysis was conducted at Ultramicroscopy center, Kyushu University.

AUTHOR DECLARATIONS

Conflict of Interest

The authors have no conflicts to disclose.

Author Contributions

The manuscript was written with the contributions of all authors. All authors have approved the final version of the manuscript

DATA AVAILABILITY

The corresponding author's data supporting this study's findings are available upon reasonable request.

REFERENCES

[1] E. Png, S. Srinivasan, K. Bekiroglu, J. Chaoyang, R. Su, and K. Poolla, Appl. Energy **239,** 408 (2019).

[2] T. Tan, Z. Yan, H. Zou, K. Ma, F. Liu, L. Zhao, Z. Peng, and W. Zhang, Appl. Energy **254,** 113717 (2019).

[3] M. Safaei, H. A. Sodano, and S. R. Anton, Smart Mater. Struct. **28,** 113001 (2019).

[4] Y. Song, C. H. Yang, S. K. Hong, S. J. Hwang, J. H. Kim, J. Y. Choi, S. K. Ryu, and T. H. Sung, Int. J. Hydrogen Energy **41,** 12563 (2016).

[5] X. Gao, J. Wu, Y. Yu, Z. Chu, H. Shi, and S. Dong, Adv. Funct. Mater. **28,** 1706895 (2018).

[6] Y. Tsujiura, E. Suwa, T. Nishi, F. Kurokawa, H. Hida, and I. Kanno, Sens. Actuators, A **261,** 295 (2017).

[7] H. C. Song, S. W. Kim, H. S. Kim, D. G. Lee, C. Y. Kang, and S. Nahm, Adv. Mater. **32,** 2002208 (2020).

[8] H. G. Yeo, X. Ma, C. Rahn, and S. Trolier-McKinstry, Adv. Funct. Mater. **26,** 5940 (2016).

[9] R. Xu and S. Kim, Proceedings of the Power MEMS**,** 464 (2012).

[10] D. Isarakorn, D. Briand, P. Janphuang, A. Sambri, S. Gariglio, J.-M. Triscone, F. Guy, J. Reiner, C. Ahn, and N. De Rooij, Smart Mater. Struct. **20,** 025015 (2011).

[11] B. A. Tuttle, J. A. Voigt, D. C. Goodnow, D. L. Lamppa, T. J. Headley, M. O. Eatough, G. Zender, R. D. Nasby, and S. M. Rodgers, J. Am. Ceram. Soc. **76**, 1537 (1993).

[12] G. L. Brennecka, W. Huebner, B. A. Tuttle, and P. G. Clem, J. Am. Ceram. Soc. **87**, 1459 (2004).

[13] K. Nashimoto, D. Fork, and G. Anderson, Appl. Phys. Lett. **66**, 822 (1995).

[14] I. Kanno, H. Kotera, and K. Wasa, Sens. Actuators, A **107**, 68 (2003).

[15]G. Tan, K. Maruyama, Y. Kanamitsu, S. Nishioka, T. Ozaki, T. Umegaki, H. Hida, and I. Kanno, Sci. Rep. **9**, 1 (2019).

[16]E. Suwa, Y. Tsujiura, F. Kurokawa, H. Hida, and I. Kanno, Energy Harvest. Syst. **3**, 61 (2016).

[17]M. Dekkers, M. D. Nguyen, R. Steenwelle, P. M. te Riele, D. H. Blank, and G. Rijnders, Appl. Phys. Lett. **95**, 012902 (2009).

[18]S. Baek, J. Park, D. Kim, V. A. Aksyuk, R. Das, S. Bu, D. Felker, J. Lettieri, V. Vaithyanathan, and S. Bharadwaja, Science **334**, 958 (2011).

[19]M.-A. Dubois and P. Muralt, Sens. Actuators, A **77**, 106 (1999).

[20]P. Muralt, R. G. Polcawich, and S. Trolier-McKinstry, MRS Bull. **34**, 658 (2009).

[21]S. V. Kalinin, B. Mirman, and E. Karapetian, Phys. Rev. B **76**, 212102 (2007).

[22]Y. Tsujiura, S. Kawabe, F. Kurokawa, H. Hida, and I. Kanno, Jpn. J. Appl. Phys. **54**, 10NA04 (2015).

[23]H. Miyabuchi, T. Yoshimura, N. Fujimura, and S. Murakami, J. Korean Phys. Soc. **59**, 2524 (2011).

[24]T. Yoshimura, K. Kariya, N. Okamoto, M. Aramaki, and N. Fujimura, J. Phys.: Conf. Ser. **1052**, 012020 (2018).

[25]S. Yoshida, H. Hanzawa, K. Wasa, and S. Tanaka, Sens. Actuators, A **239**, 201 (2016).

[26]M. D. Nguyen, E. Houwman, M. Dekkers, D. Schlom, and G. Rijnders, APL Mater. **5**, 074201 (2017).

[27]K. Saito, T. Kurosawa, T. Akai, T. Oikawa, and H. Funakubo, J. Appl. Phys. **93**, 545 (2003).

[28]Y. Ehara, S. Yasui, T. Oikawa, T. Shiraishi, T. Shimizu, H. Tanaka, N. Kanenko, R. Maran, T. Yamada, and Y. Imai, Sci. Rep. **7**, 1 (2017).

[29]M. A. Hopcroft, W. D. Nix, and T. W. Kenny, J. Microelectromech. Syst. **19**, 229 (2010).

[30]S. Yoshida, H. Hanzawa, K. Wasa, M. Esashi, and S. Tanaka, IEEE Trans. Ultrason., Ferroelectr. Freq. Control **61**, 1552 (2014).

[31]N. Ledermann, P. Muralt, J. Baborowski, S. Gentil, K. Mukati, M. Cantoni, A. Seifert, and N. Setter, Sens. Actuators, A **105**, 162 (2003).

[32]J. Ouyang, R. Ramesh, and A. Roytburd, Appl. Phys. Lett. **86**, 152901 (2005).

[33]S. O. Isikman, O. Ergeneman, A. D. Yalcinkaya, and H. Urey, IEEE J. Sel. Top. Quantum Electron. **13**, 283 (2007).

[34]K. Coleman, R. Bermejo, D. Leguillon, and S. Trolier-McKinstry, Acta Mater. **191**, 245 (2020).

[35]K. Morimoto, I. Kanno, K. Wasa, and H. Kotera, Sens. Actuators, A **163**, 428 (2010).

[36]K. Wasa, T. Matsushima, H. Adachi, I. Kanno, H. Kotera, J. Microelectromech. Syst. **21**, 451 (2012).

[37]S. Trolier-McKinstry, F. Griggio, C. Yaeger, P. Jousse, D. Zhao, S.S. Bharadwaja, T.N. Jackson, S. Jesse, S.V. Kalinin, K. Wasa, IEEE Trans. Ultrason., Ferroelectr. Freq. Control **58**, 1782 (2011).

[38]C. B. Yeager, Y. Ehara, N. Oshima, H. Funakubo, and S. Trolier-McKinstry, J. Appl. Phys. **116**, 104907 (2014).

FIGURES

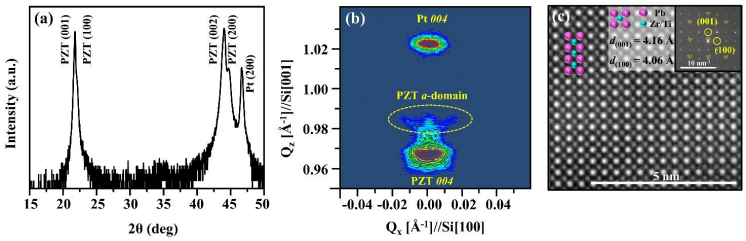

FIG. 1. (a) XRD pattern and (b) XRD reciprocal space map (RSM) around the PZT *004* reflection and (c) enlarged high-resolution scanning transmission electron microscopy (HRSTEM) image of the PZT thin film grown on (001)SRO/Pt/ZrO_2/Si substrate. The inset shows the electron diffraction pattern.

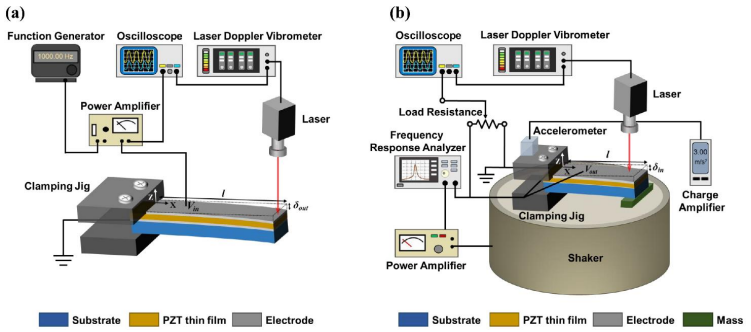

FIG. 2. Schematic representations of measurement setup of the effective transverse piezoelectric coefficients ($e_{31,f}$) from the (a) converse piezoelectric effect and (b) direct piezoelectric effect.

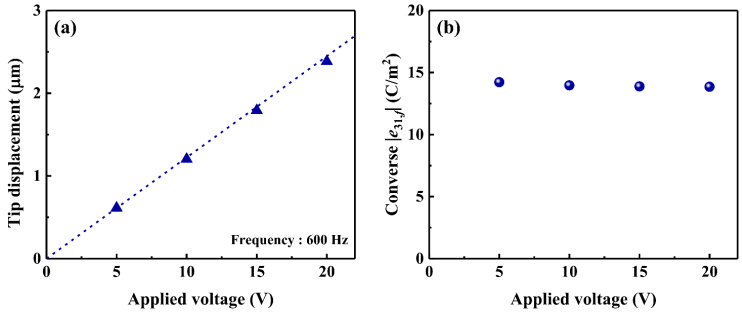

FIG. 3. (a) Output tip displacement of the epitaxial PZT/Si cantilever as a function of applied voltage. (b) The effective transverse piezoelectric coefficient $|e_{31,f}|$ of the epitaxial PZT/Si cantilever evaluated from the converse piezoelectric effect.

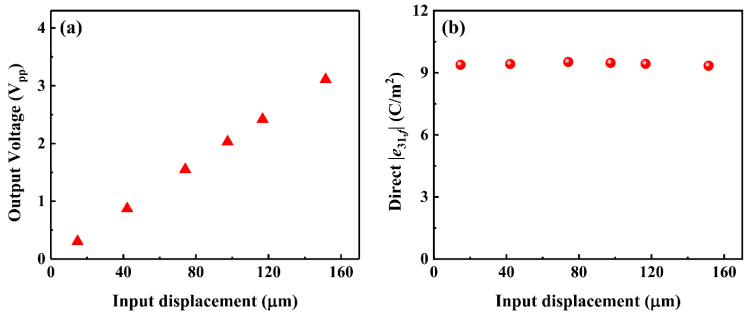

FIG. 4. (a) Output voltage of the epitaxial PZT/Si cantilever as a function of input displacement. (b) The effective transverse piezoelectric coefficient $|e_{31,f}|$ of the epitaxial PZT/Si cantilever evaluated from the direct piezoelectric effect.

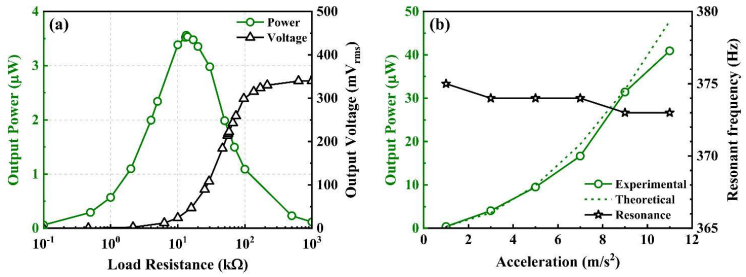

FIG. 5. (a) Output power and voltage of PEH using epitaxial PZT/Si cantilever as a function of load resistance at a resonant frequency and with an acceleration of 3 m/s^2. (b) The output power with an optimal load resistance at a resonant frequency as a function of acceleration.

TABLE

TABLE I. Typical dielectric and piezoelectric coefficients of PZT-based thin films.

Thin film	**PZT**	PMnN-PZT	PZT	PZT	PZT	PZT	PZT
Substrate	**Si**	Si	Si	MgO	Si	Si	Si
Crystal structure	**Epitaxial**	Epitaxial	Epitaxial	Epitaxial	Epitaxial	Polycrystal	Polycrystal
$\varepsilon_{r,33}$	**318**	~200	~220	100 to 200	~700	550	680
Converse $\lvert e_{31,f}\rvert$ [C/m^2]	**14.0–14.3**	14.0	10.9	6 to 10	-	11.5–15.0	6.7
Converse FOM [GPa]	**70–73**	~110	~60	20 to 110	-	27–46	7
Direct $\lvert e_{31,f}\rvert$ [C/m^2]	**9.4**	-	-	-	12.0	6.4	-
Direct FOM [GPa]	**32**	-	-	-	~23	9	-
Measurement method	**Cantilever method (Energy harvesting system for direct $\lvert e_{31,f}\rvert$)**	Cantilever method	Cantilever method	Cantilever method	Wafer flexure method	Cantilever method	Cantilever method
Reference	**This study**	25	30	36, 37	38	22	31

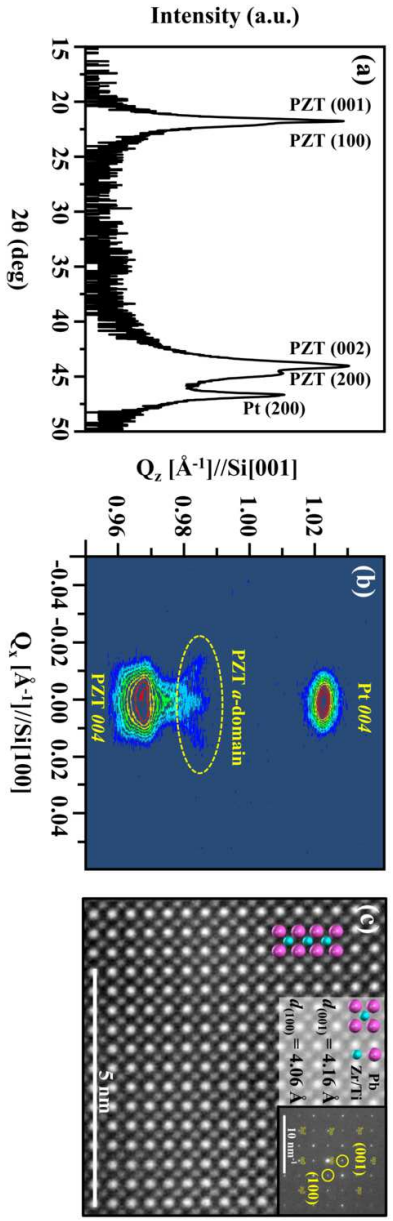

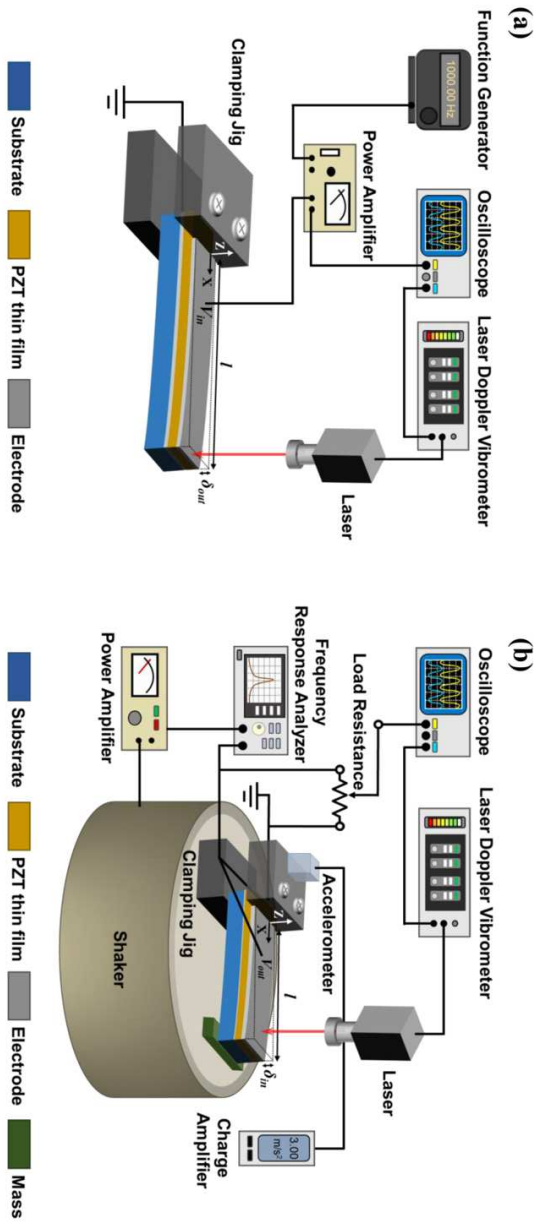

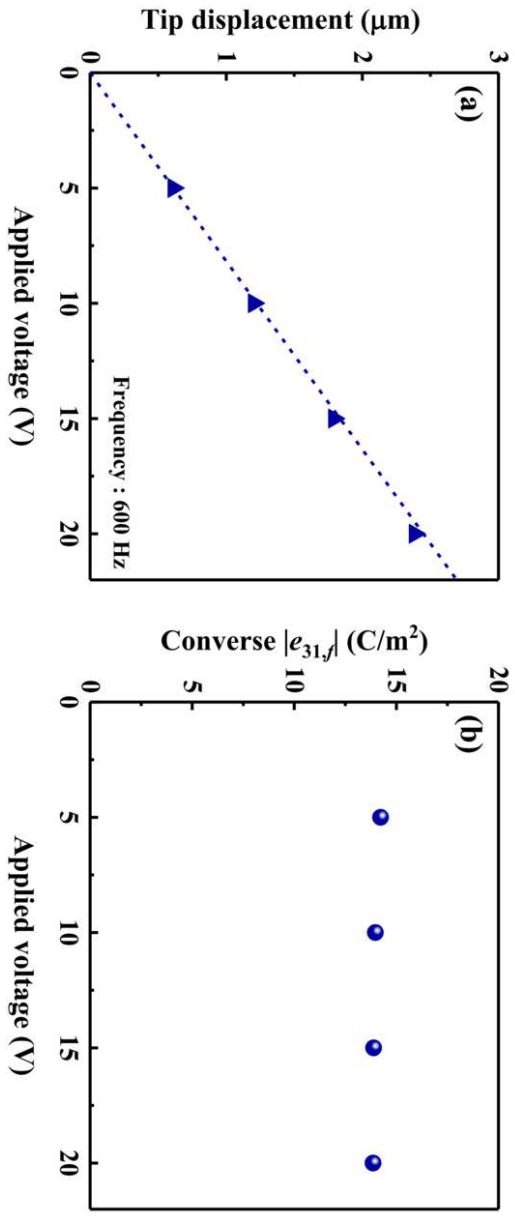

PLEASE CITE THIS ARTICLE AS DOI: 10.1063/5.0105103